Journal of Oral Biosciences 61 (2019) 43–54

Contents lists available at ScienceDirect

Journal of Oral Biosciences

journal homepage: www.elsevier.com/locate/job

Potential function of TGF-β isoforms in maturation-stage ameloblasts

Miu Okubo[a], Risako Chiba[b], Takeo Karakida[b], Hajime Yamazaki[c,d,1], Ryuji Yamamoto[b], Saeko Kobayashi[e], Takahiko Niwa[a], Henry C. Margolis[c,d,2], Takatoshi Nagano[a], Yasuo Yamakoshi[b,*], Kazuhiro Gomi[a]

[a] Department of Periodontology, School of Dental Medicine, Tsurumi University, 2-1-3 Tsurumi, Tsurumi-ku, Yokohama 230-8501, Japan
[b] Department of Biochemistry and Molecular Biology, School of Dental Medicine, Tsurumi University, 2-1-3 Tsurumi, Tsurumi-ku, Yokohama 230-8501, Japan
[c] The Forsyth Institute, 245 First Street, Cambridge, Boston, MA 02142, USA
[d] Department of Development Biology, Harvard School of Dental Medicine, 188 Longwood Avenue, Boston, MA 02115, USA
[e] Department of Pediatric Dentistry, School of Dental Medicine, Tsurumi University, 2-1-3 Tsurumi, Tsurumi-ku, Yokohama 230-8501, Japan

ARTICLE INFO

Article history:
Received 19 November 2018
Received in revised form
18 December 2018
Accepted 19 December 2018
Available online 3 January 2019

Keywords:
Enamel
Ameloblast
Transforming growth factor-beta
Apoptosis
Endocytosis

ABSTRACT

Objectives: To investigate potential functions of transforming growth factor-beta (TGF-β) isoforms in maturation-stage ameloblasts during amelogenesis.
Methods: In vivo activation of TGF-β was characterized by using matrix metalloproteinase 20 null (*Mmp20*$^{-/-}$) and wild-type (*Mmp20*$^{+/+}$) mice. Using mHAT9d cells cultured in the presence of each TGF-β isoform, (1) cell proliferation was determined by MTS assay, (2) immunostaining with anti-cleaved caspase-3 monoclonal antibody was performed and apoptotic indices were measured, (3) gene expression was analyzed by RT-qPCR, and (4) the uptake of amelogenin into mHAT9d cells was directly observed using a fluorescence microscope.
Results: TGF-β1 and TGF-β3 were present in the enamel matrix of developing teeth which were activated by MMP20 *in vivo*. A genetic study revealed that the three TGF-β isoforms upregulate kallikrein 4 (KLK4) mRNA levels but downregulate carbonic anhydrase II. Moreover, TGF-β1 and TGF-β2 significantly upregulated the mRNA level of amelotin, whereas TGF-β3 dramatically downregulated the mRNA levels of odontogenic ameloblast-associated protein (ODAM), family with sequence similarity 83 member H (FAM83H), and alkaline phosphatase (ALP). Immunostaining analysis showed that the apoptosis of mHAT9d cells is induced by three TGF-β isoforms, with TGF-β3 being most effective. Both TGF-β1 and TGF-β3 induced endocytosis of amelogenin.
Conclusions: We propose that TGF-β is regulated in an isoform-specific manner to perform multiple biological functions such as gene expression related to the structure of basal lamina/ameloblasts, mineral ion transport, apoptosis, and endocytosis in maturation-stage ameloblasts.

1. Introduction

Enamel formation progresses through three developmental stages: secretion, transition, and maturation. During these three stages, enamel proteins are secreted, proteolytically processed, degraded, and reabsorbed into ameloblasts while ions are exchanged between ameloblasts and the developing extracellular matrix [1,2]. Enamel proteins are secreted from the Tomes' processes of the secretory-stage ameloblasts and are abundant in the extracellular matrix during the secretory and early maturation

Abbreviations: EDTA, ethylenediaminetetraacetic acid; CD63, lysosome-associated membrane glycoprotein-3; GAPDH, glyceraldehyde-3-phosphate dehydrogenase; HRP, horseradish peroxidase; IgG, immunoglobulin G; MC3T3-E1, mouse osteoblastic cell line; MTS, 3-[4,5,dimethylthiazol-2-yl]-5-[3-carboxymethoxy-phenyl]-2-[4-sulfophenyl]-2H-tetrazolium inner; PAGE, polyacrylamide gel electrophoresis; TUNEL, TdT-mediated dUTP nick and labeling; Smad, the homologies to the *Caenorhabditis elegans* SMA ("small" worm phenotype) and *Drosophila* MAD ("Mothers Against Decapentaplegic") family of genes

* Corresponding author.
E-mail addresses: okubo-miu@tsurumi-u.ac.jp (M. Okubo), chiba-r@tsurumi-u.ac.jp (R. Chiba), karakida-t@tsurumi-u.ac.jp (T. Karakida), yamamoto-rj@tsurumi-u.ac.jp (R. Yamamoto), kinoshita-saeko@tsurumi-u.ac.jp (S. Kobayashi), niwa-takahiko@tsurumi-u.ac.jp (T. Niwa), nagano-takatoshi@tsurumi-u.ac.jp (T. Nagano), yamakoshi-y@tsurumi-u.ac.jp (Y. Yamakoshi), gomi-k@tsurumi-u.ac.jp (K. Gomi).
[1] **Present address:** Department of Oral Biology, University of Pittsburgh School of Dental Medicine, 3501 Terrace Street, Pittsburgh, PA 15261, USA.
[2] **Present address:** Department of Periodontics/Preventative Medicine, University of Pittsburgh School of Dental Medicine, 3501 Terrace Street, Pittsburgh, PA 15261, USA.

https://doi.org/10.1016/j.job.2018.12.002
1349-0079/

stages. These enamel proteins eventually diminish from the matrix and are present in trace amounts by the late maturation stage. The degradation and removal of enamel proteins progress through the action of proteases and cleaved proteins, and/or reabsorption of small fragments from the matrix *via* endocytosis by maturation-stage ameloblasts [3].

Following internal reorganization of ameloblasts during the transition stage, a specialized basal lamina forms along the distal membrane of maturation-stage ameloblasts, which varies between ruffle-ended and smooth-ended forms [4]. Although approximately 50% of ameloblasts undergo apoptosis during both the transition and maturation stages [5], maturation-stage ameloblasts synthesize proteins and enzymes associated with the structure of the basal lamina and the transport of mineral ions, finally increasing width and thickness of the enamel crystallites.

Transforming growth factor-beta (TGF-β) induces proliferation, differentiation, chemotaxis, and apoptosis in monocytes and in epithelial, mesenchymal, and neuronal cells [6]. TGF-β1, TGF-β2, and TGF-β3 exhibit similar biological activities in mammals [7,8]. In pigs, the active-form of TGF-β1 is present in the extracellular matrix of secretory-stage enamel [9], and is activated by enamelysin (MMP20) *in vitro* [10]. The activated TGF-β1 binds to water-soluble amelogenin cleavage products to maintain its activity. The amelogenin-TGF-β1 complex binds to the TGF-β receptor moving in the liquid phase and regulates multiple events not only in secretory-stage ameloblasts but also in transition- and maturation-stage ameloblasts *via* autocrine signal transduction [10].

In this study, we evaluated the different functions of TGF-β isoforms, focusing on the stages beyond the secretory phase. We investigated *in vivo* activation, cell proliferation, apoptosis, gene expression, and endocytosis at the protein, histological, and genetic levels.

2. Materials and methods

2.1. MMP20 knockout mouse and genotyping

Mmp20(+/-) mice with C57BL/6 and P129 backgrounds were purchased from the Mutant Mouse Regional Resource Center (Columbia, MO) and bred to generate wild-type [*Mmp20*(+/+)], heterozygous [*Mmp20*(+/-)], and null [*Mmp20*(-/-)] strains. Mice were genotyped at 4-weeks of age, as previously described [11].

2.2. Enzyme assay (ALP-HPDL system)

Human periodontal ligament cells (HPDLs) were purchased from Lonza (Lonza, Walkersville, MD, USA). Cell culture and ALP activity assays were performed based on our previous method [9].

2.3. Enzyme-linked immunosorbent assay (ELISA)

TGF-β1, TGF-β2 and TGF-β3 in protein samples extracted from the first molars of $Mmp20^{+/+}$, $Mmp20^{+/-}$ and $Mmp20^{-/-}$ mice at days 5 and 11 were evaluated with a sandwich enzyme immunoassay method using a Quantikine ELISA kit (R&D Systems, Inc., Minneapolis, MN, USA).

2.4. Cell proliferation assay

The proliferation rate of mHAT9d cells using six 96-well plates was determined on days 0, 1 and 2 by the CellTiter 96® AQuous One Solution Cell Proliferation Assay (MTS assay) (Promega Corporation, Madison, WI, USA) [12].

2.5. Reverse transcription quantitative polymerase chain reaction (RT-qPCR)

RT-qPCR of the total RNA prepared from mHAT9d cells or murine enamel organ epithelium was performed using the SYBR Green technique on a LightCycler Nano system (Roche Diagnostics, Mannheim, Germany). The specific primer sets and reaction conditions are shown in Appendix Table A1.

2.6. Assessment of apoptosis by immunohistochemistry

On day 10, after culturing in the absence or presence of TGF-β isoforms, mHAT9d cells on chamber slides were immunostained with anti-cleaved caspase-3 monoclonal antibody. The apoptosis of mHAT9d cells was assessed by the apoptotic index, calculated as the percentage of the whole mHAT9d cell population [12].

2.7. Preparation of fluorescent-labeled amelogenin

The P103 amelogenin, which is a cleavage product of P173 original amelogenin, was purified from 5-month-old porcine second molar by using our previous method [10,13]. The purified P103 amelogenin was fluorescent-labeled with HyLyte Fluor 647 labeling Kit (Dojindo Molecular Technologies, Inc., Rockville, MD, USA). After the removal of excess dye with PD-10 column (GE Healthcare, Chicago, IL, USA), the HyLyte Fluor 647-labeled P103 amelogenin was finally purified by reverse phase-high performance liquid chromatography using a Discovery C18 column.

2.8. Uptake of amelogenin-cleaved products into mHAT9d cells

The HyLyte Fluor 647-labeled P103 amelogenin was added to subconfluent mHAT9d cells (1.0×10^3 cells/well in a 96 well plate) at a final concentration of 1 mg/mL. Following a 1–2 h incubation in the presence or absence of TGF-β isoforms, the uptake of amelogenin was observed using a fluorescent microscope (Biozero BZ-8100, Keyence, Osaka, Japan).

2.9. Statistical analysis

For ELISA and enzyme assays with the ALP-HPDL system, all values are presented as the mean ± s.e.m. Statistical significance was determined using an unpaired Student t-test for ELISA and ALP-HPDL, a Steel-Dwass test for the MTS assay and a RT-qPCR analysis and Mann-Whitney U test for apoptosis indices. In all cases, $p < 0.001$, $p < 0.01$ or $p < 0.05$ were regarded as statistically significant.

3. Results

3.1. Activation of TGF-β by MMP20 in vivo

By using $Mmp20^{+/+}$, $Mmp20^{+/-}$ and $Mmp20^{-/-}$ mice and the ALP-HPDL system, we determined the *in vivo* TGF-β activity. We initially observed mandibular incisor morphology in 3-month-old $Mmp20^{+/+}$ and $Mmp20^{-/-}$ mice using backscattered scanning electron microscopy (bSEM) (Appendix Fig. A1) and characterized enamel proteins extracted from the first molars of $Mmp20^{+/+}$, $Mmp20^{+/-}$ and $Mmp20^{-/-}$ mice at days 5 and 11 (Appendix Fig. A2).

After confirming that above results were consistent with the previous data [14,15], we determined ALP-inducing activity in HPDL cells of the enamel extracts. The activity of TGF-β significantly differed among $Mmp20^{+/+}$, $Mmp20^{+/-}$ and $Mmp20^{-/-}$ mice (Fig. 1A). Both day-5 and day-11 protein samples from mice of all the genotypes showed enhanced ALP-inducing activity, but

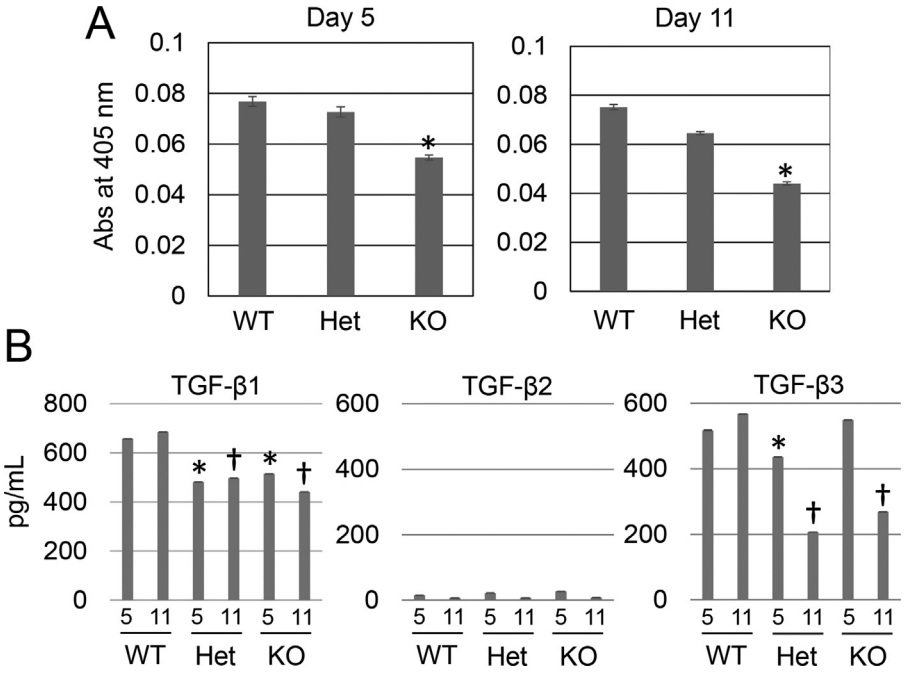

Fig. 1. Detection of TGF-β at days 5 (5) and 11 (11) in wild-type (WT), matrix metalloproteinase 20 (*Mmp20*) heterozygous (Het) and *Mmp*20 null (KO) mice. **(A)** ALP-inducing activity of HPDL cells exposed to protein fractions at day 5 (left) and day 11 (right) (n = 6). The asterisk (*) on the bar graph indicates a significant difference between the WT and KO samples. Values are expressed as the mean ± s.e.m. ($^{*}p < 0.05$, Student's t-test). **(B)** ELISA for the detection of TGF-β isoforms: TGF-β1 (left), TGF-β2 (middle) and TGF-β3 (right) (n = 6). On the bar graph, a significant difference from WT values is indicated with an asterisk (*) for day 5 mice and a dagger (†) for day 11 mice. Values are expressed as the mean ± s.e.m. ($^{*}p < 0.05$ and $^{\dagger}p < 0.05$, Student's t-test).

the intensity of ALP-inducing activity in the *Mmp20*$^{-/-}$ mice was approximately 1.4–1.7-fold lower than that in *Mmp20*$^{+/+}$ mice. Fig. 1B shows ELISA results using TGF-β1, TGF-β2 and TGF-β3 antibodies (Appendix Fig. A3). Both TGF-β1 and TGF-β3 were predominantly detected in the protein samples of all the genotypes, but TGF-β2 was barely detected. Interestingly, the concentrations of TGF-β1 and TGF-β3 in the *Mmp20*$^{+/-}$ and *Mmp20*$^{-/-}$ mice were significantly lower than those in the *Mmp20*$^{+/+}$ mice. In addition, the amount of TGF-β3 in the *Mmp20*$^{+/-}$ and *Mmp20*$^{-/-}$ mice was significantly different between day 5 and day 11.

3.2. Proliferation rate of mHAT9d cells

Because TGF-β is activated by MMP20 *in vivo*, we investigated the *in vivo* function of the active-form of TGF-β during amelogenesis using a dental epithelial cell line derived from the apical bud of a mouse incisor (mHAT9d) [16] and the effects of TGF-β isoforms on cell proliferation (Fig. 2A). We previously determined that the maximum effective concentration of human recombinant TGF-β1 for HPDL cells is 1 ng/mL (Appendix Fig. A4). Based on these data and the supplier's product data sheet, we decided to use 1 ng/mL of each TGF-β isoform for subsequent cell experiments. Compared to day 0 (before the start of culture), the proliferation rate of cells cultured in the absence of TGF-β isoforms (*i.e.*, control cells) increased by 2.68-fold at day 2. Culturing cells in the presence of TGF-β isoforms also increased the rate of proliferation (2.21-fold for TGF-β1, 2.05-fold for TGF-β2 and 1.53-fold for TGF-β3 at day 2), but these cell growth rates were suppressed compared to that of the control, in particular, the effect of TGF-β3 was remarkable. Moreover, the cell population doubling time in the presence of the TGF-β isoforms increased in the order of TGF-β3 >> TGF-β2 > TGF-β1 (Fig. 2B).

3.3. Expression of enamel-formation-related genes in mHAT9d cells

We investigated whether TGF-β isoforms affect the mRNA expression of enamel-formation-related genes in mHAT9d cells (Fig. 3). For RT-qPCR analysis, day 10 of culture, when the cells reached confluence after being exposed to the various conditions, was chosen as the measurement time point. Using RT-qPCR, primer sets that we designed (Appendix Table A1) and total RNA isolated from mHAT9d cells at day 10 after culture in the presence or absence of each TGF-β isoform, we quantified the mRNA expression levels of amelogenin (*Amel*), enamelin (*Enam*), ameloblastin (*Ambn*) and enamelysin (*Mmp20*) as marker genes for s ecretory-stage ameloblasts, and amelotin (*Amtn*), odontogenic ameloblast-associated protein (*Odam*), kallikrein 4 (*Klk4*), carbonic anhydrase (*Car2*) and V-type proton ATPase (*Atp6v1e1*) as marker genes for maturation-stage ameloblasts. We also measured the mRNA expression levels of family with sequence similarity 83 member H (*Fam83h*), WD repeat-containing protein 72 (*Wdr72*), and alkaline phosphatase (*Alp*). Compared to the control cells grown in the absence of TGF-β, three TGF-β isoforms significantly upregulated the mRNA level of *Klk4* (5.83-fold for TGF-β1, 5.17-fold for TGF-β2 and 5.29-fold for TGF-β3), but significantly downregulated that of *Car2* (1.47-fold for TGF-β1, 1.43-fold for TGF-β2 and 3.33-fold for TGF-β3). Both TGF-β1 and TGF-β2 enhanced the mRNA level of *Amtn* (2.31-fold for TGF-β1 and 2.35-fold for TGF-β2), but they did not affect the mRNA levels of *Odam*, *Fam83h*, *Wdr72*, *Alp* and *Atp6v1e1*. Interestingly, TGF-β3 significantly downregulated *Odam* (3.77-fold), *Fam83h* (3.18-fold), *Wdr72* (3.69-fold) and *Alp* (5.74-fold) but had no effect on *Atp6v1e1*. The expression of marker genes for secretory-stage ameloblasts, namely, *Amel*, *Enam*, *Ambn* and *Mmp20*, was barely detected in the mHAT9d cells used in this study. In Table 1, we summarize the effect of the TGF-β isoforms on the expression of related genes for maturation-stage-ameloblasts in the mHAT9d cells.

3.4. Apoptosis of mHAT9d cells

As the RT-qPCR analysis was carried out at day 10 after culture, we also performed the apoptosis experiment at the same time point.

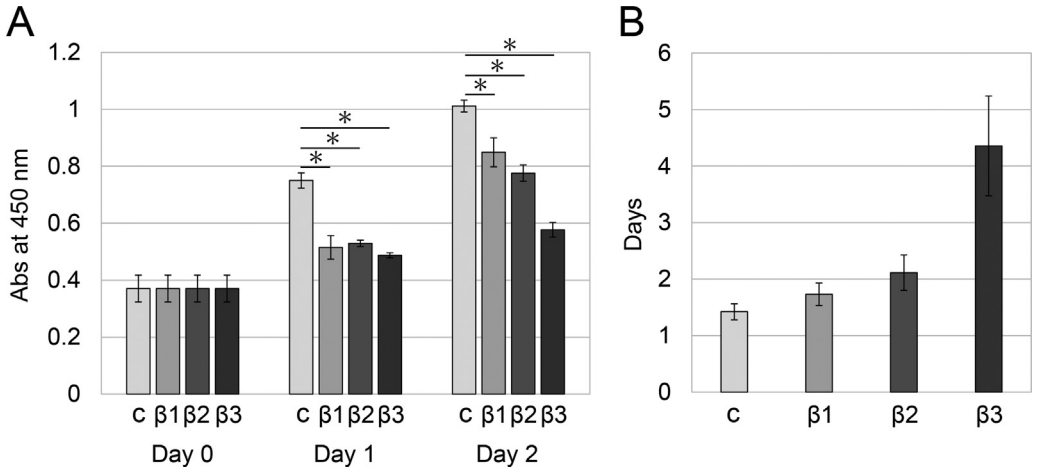

Fig. 2. Effect of TGF-β isoforms on the proliferation of mHAT9d cells. **(A)** MTS assay. Cells in the absence (c) or presence of TGF-β1 (β1), TGF-β2 (β2) and TGF-β3 (β3) on day 0, 1 and 2 were cultured at a final volume of 120 μL/well for 1 h at 37 °C. MTS reagent was added, and an absorbance of 450 nm was recorded using a microplate reader (n = 8 tests per sample). Values are expressed as the mean ± s.e.m. (*$p < 0.01$, Steel-Dwass test). **(B)** Cell population doubling time against days after cell culture in the absence (c) or presence of TGF-β1 (β1), TGF-β2 (β2) and TGF-β3 (β3). Cell population doubling time was calculated by a regression curve. Data are means ± s.e.m.

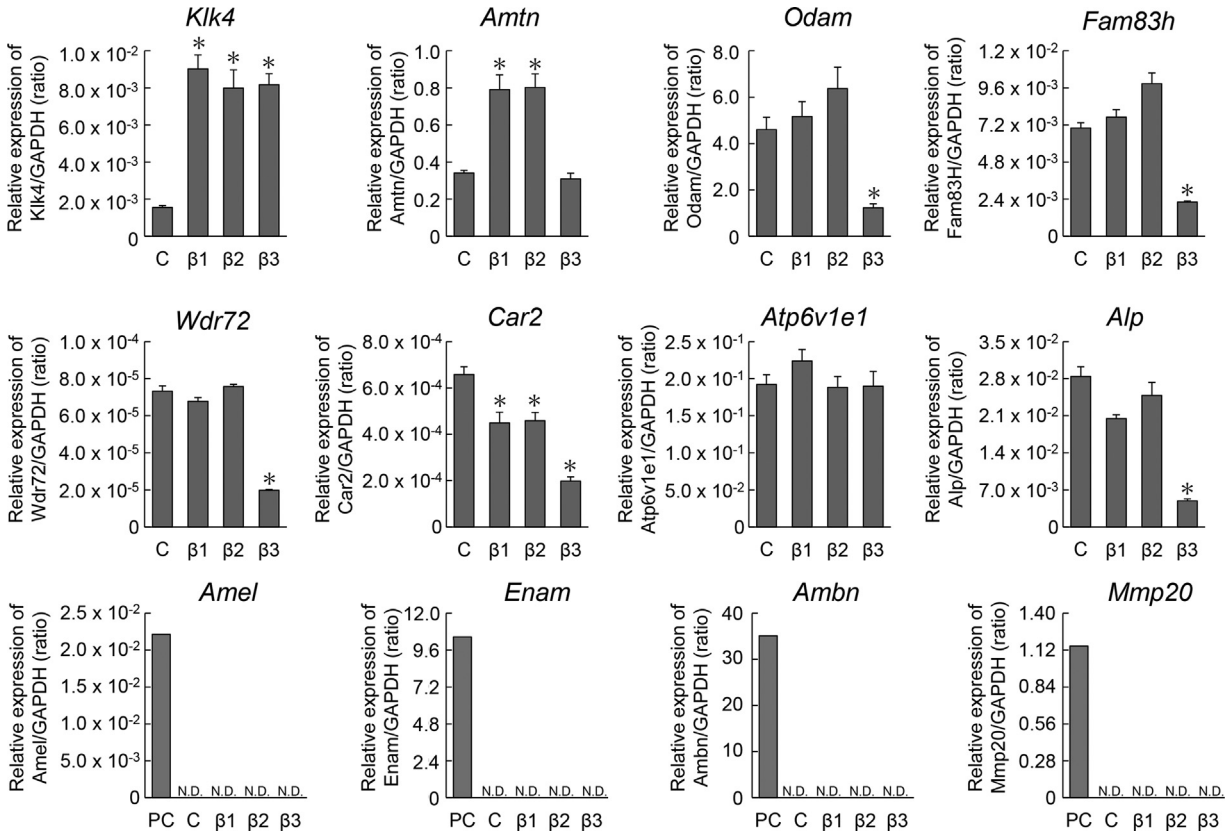

Fig. 3. Effect of TGF-β isoforms on gene expression in mHAT9d cells. RT-qPCR analysis at day 10 after culture in the absence (C) or presence of TGF-β1 (β1), TGF-β2 (β2) and TGF-β3 (β3). *Klk4*: kallikrein 4, *Amtn*: amelotin, *Odam*: odontogenic ameloblast-associated protein, *Fam83H*: family with sequence similarity 83 member H, *Wdr72*: WD repeat-containing protein 72, *Car2*: carbonic anhydrase II, *Atp6v1e1*: V-type proton ATPase, *Alp*: alkaline phosphatase, *Amel*: amelogenin, *Enam*: enamelin, *Ambn*: ameloblastin and *Mmp20*: enamelysin. PC: the total RNA prepared from enamel organ epithelium of day 5 mouse first molars. N.D: not determined. Each mRNA expression value was normalized to that of the reference gene glyceraldehyde-3-phosphate dehydrogenase (*Gapdh*), and the relative quantification data for *Klk4*, *Amtn*, *Odam*, *Fam83H*, *Wdr72*, *Car2*, *Atp6v1e1*, *Alp*, *Amel*, *Enam*, *Ambn* and *Mmp20* in mHAT9d cells were generated on the basis of a mathematical model for relative quantification in a RT-qPCR system (n = 6). All values are presented as the mean ± s.e.m. (*$p < 0.05$, Steel-Dwass test).

Apoptotic bodies were observed in hematoxylin-eosin (HE)-stained sections from mHAT9d cells cultured with or without each of the TGF-β isoforms (Fig. 4A). Eosinophilic apoptotic bodies as detected by light microscopy in HE-stained mHAT9d sections are shown in Fig. 4A. The same mHAT9d cells were used for an immunohistochemical study of cleaved caspase-3-positive cells. Compared to the negative controls, putative preapoptotic cells were observed to be stained brown and were characterized by a positive

Table 1
Effect of TGF-β isoforms on gene expression of related genes for maturation-stage ameloblasts in mHAT9d cells.

	TGF-β1	TGF-β2	TGF-β3
Klk4	↑	↑	↑
Amtn	↑	↑	→
Odam	→	→	↓
Fam83h	→	→	↓
Wdr72	→	→	↓
Car2	↓	↓	↓
Alp	→	→	↓
Atp6v1e1	→	→	→

Note: Arrow indicates ↑: up-regulation, ↓: down-regulation and →: no effect.

antibody-reaction with mainly cytoplasmic localization. We further quantitated the occurrence of cleaved caspase-3-positive cells. The total number of caspase-3-positive apoptotic events for four groups were counted, and the apoptotic indices (AIs) calculated for the different treatment groups are shown in Fig. 4B. Approximately, 3% of caspase-3-labeled cells were detected in the control (3.11 ± 0.32%). The AIs of the TGF-β-treated mHAT9d cells were 5.41 ± 0.76% for TGF-β1, 6.98 ± 0.94% for TGF-β2, and 11.29 ± 1.12% for TGF-β3. Compared to the control AIs, the AIs in the TGF-β-treated mHAT9d cells were significantly higher (approximately 1.74-fold for TGF-β1, 2.24-fold for TGF-β2, and 3.63-fold for TGF-β3).

3.5. Uptake of amelogenin-cleaved products into mHAT9d cells

As enamel proteins undergoing proteolytic cleavage are removed from the matrix *via* endocytosis by ameloblasts [17], we examined whether TGF-β is involved in the endocytic activity of mHAT9d cells. To perform this experiment, we initially purified a water-soluble amelogenin (P103 amelogenin) from 5-month-old porcine second molars and fluorescence-labeled it with HiLyte Fluor 647 (Appendix Fig. A5). In living mHAT9d cells, HiLyte Fluor 647-labeled P103 amelogenin was found to be distributed in the cytosol (Fig. 5). Imaging at 1 and 2 h after the uptake revealed that both TGF-β1 and TGF-β3 enhanced the fluorescence intensity of HiLyte Fluor 647-labeled P103 amelogenin, compared to that of the control without TGF-β treatment (Fig. 5A). Treatment with TGF-β2 also slightly increased the fluorescence intensity (Fig. 5A). We further attempted to confirm that the protein up taken by mHAT9d cells was indeed P103 amelogenin by using immunofluorescence staining. Following 6.5 h of TGF-β1 treatment, cells were collected and stained with 4',6-diamidino-2-phenylindole dihydrochloride (DAPI) and an Alexa Fluor 488-labeled anti-amelogenin antibody. When we combined the image of DAPI staining the nuclei of all fixed mHAT9d cells (Fig. 5B) and the Alexa Fluor 488 filtered image corresponding to the location of P103 amelogenin (Fig. 5B), the merged image revealed that P103 amelogenin was mainly localized in the cytosol of mHAT9d cells (Fig. 5B). The image of Alexa Fluor 488 was consistent with that of HiLyte Fluor 647, as described above. The fluorescence intensity of TGF-β1 and TGF-β3 at 1 h was

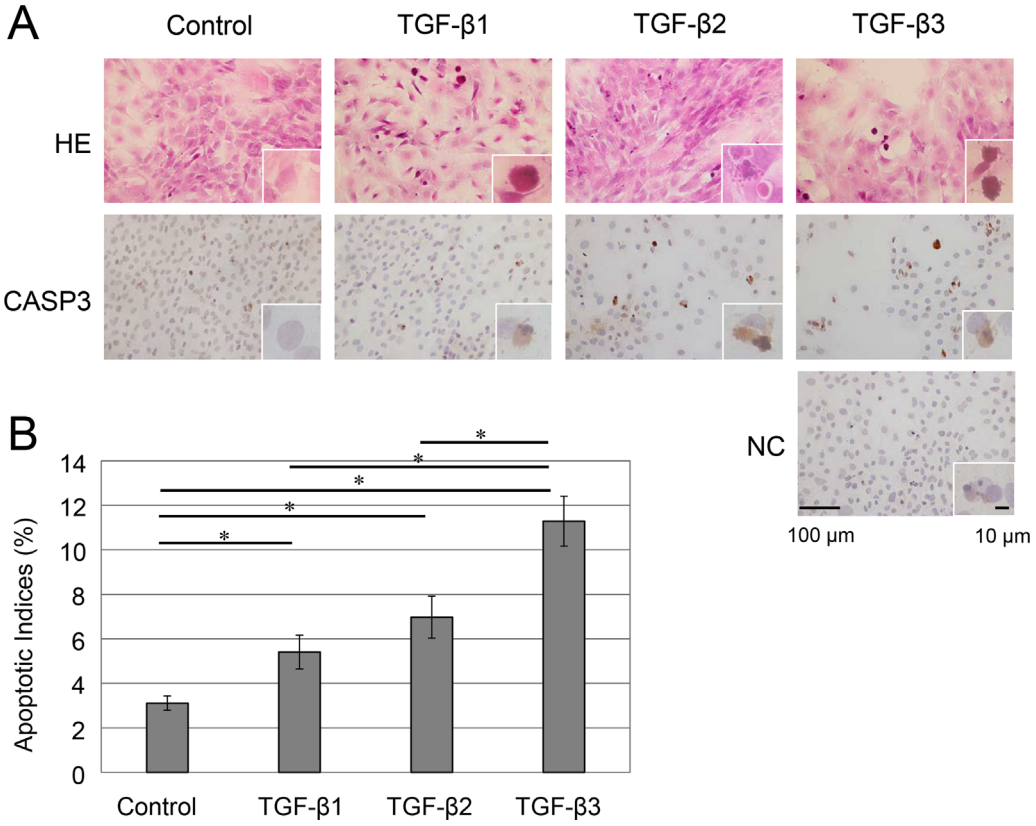

Fig. 4. Effect of TGF-β isoforms on apoptosis in mHAT9d cells. **(A)** Immunohistochemical detection of apoptosis and **(B)** apoptotic indices in mHAT9d cells on day 10 following culture in the absence (Control) or presence of TGF-β1, TGF-β2 and TGF-β3. **(A)** Eosinophilic apoptotic bodies in hematoxylin-eosin-stained mHAT9d cells detected by transmitted-light microscopy (HE) (magnification: 200 ×). Apoptotic bodies in mHAT9d cells stained by cleaved caspase-3 antibody (CASP3); the control was processed without a primary antibody (NC). The images are a high magnification (400 ×) of the area boxed in the Figure. **(B)** Apoptotic indices in mHAT9d cells. Each of the apoptotic indices was calculated as the percentage of the whole mHAT9d cell population (n = 15). Values are expressed as the mean percentage ± s.e.m. (*$p < 0.001$, Mann-Whitney U test).

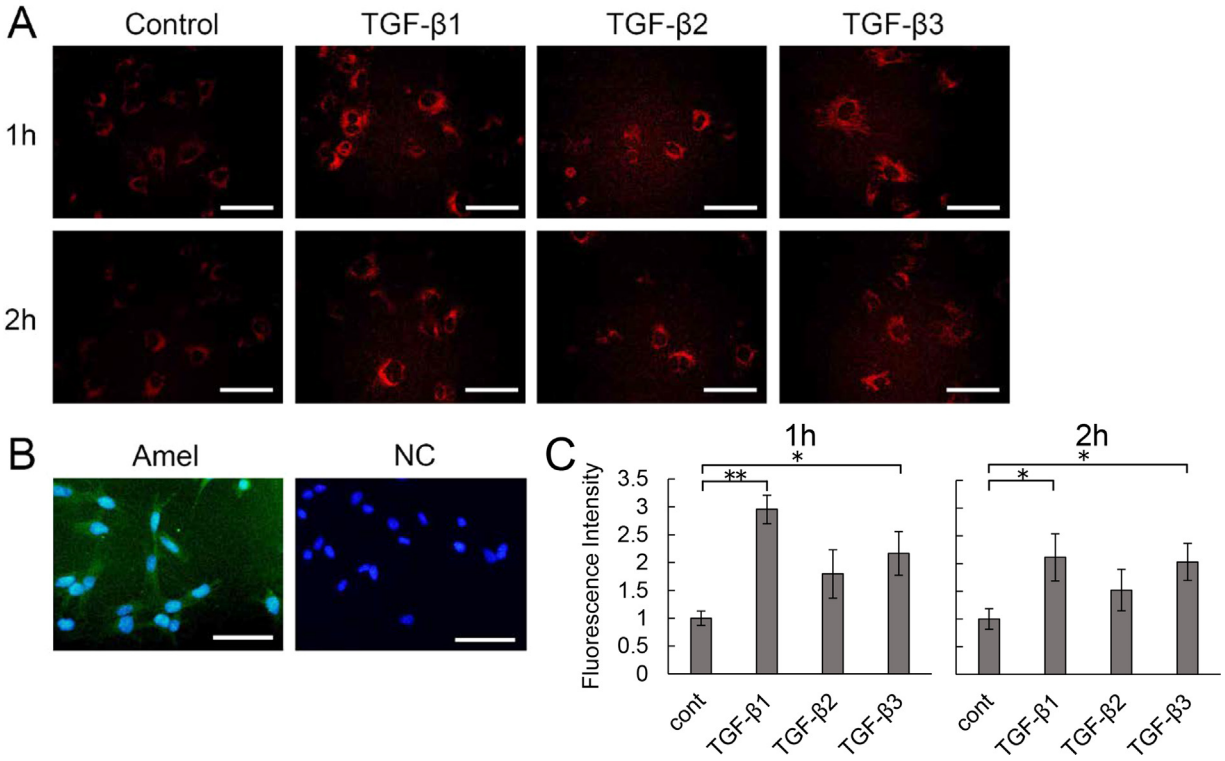

Fig. 5. Effect of TGF-β isoforms on the uptake of P103 amelogenin into mHAT9d cells. **(A)** Fluorescence detection of HyLyte Fluor 647-labeled P103 amelogenin into mHAT9d cells at 1 and 2 h following uptake in the absence (Control) or presence of TGF-β1, TGF-β2 and TGF-β3 (scale bar, 100 μm). **(B)** Immunofluorescence analysis of amelogenin in mHAT9d cells at 6.5 h following culture in the presence of amelogenin (Amel) or in the absence of amelogenin (NC) without the addition of TGF-β isoforms. Detection of amelogenin (green) in fixed mHAT9d cells was carried out by using a mouse amelogenin antibody at a dilution of 1:500 and an Alexa Fluor 488-conjugated rabbit anti-mouse antibody at a dilution of 1:500. DAPI was used to stain the cell nuclei (blue) at a concentration of 2 μg/mL (scale bar, 100 μm). **(C)** Quantification analyses of uptake of HyLyte Fluor 647-labeled P103 amelogenin into mHAT9d cells at 1 and 2 h following uptake in the absence (Cont) or presence of TGF-β1, TGF-β2 and TGF-β3. The fluorescence intensity of cells (n = 6) was calculated in the same specified range (0.5 cm × 0.5 cm) by using ImageJ software and normalized the fluorescence intensity of control as 1. Values are expressed as the mean percentage ± s.e.m. ($^{*}p < 0.05$, $^{**}p < 0.01$ Student-t test).

significantly higher (2.9-fold for TGF-β1 and 2.1-fold for TGF-β3) than that of control. The fluorescence intensity of TGF-β2 also showed a tendency to increase, but there was no significant difference with respect to control. At 2 h, the fluorescence intensity against control of TGF-β1 was reduced (2.1-fold), but that of TGF-β3 was maintained (2.0-fold) (Fig. 5C).

4. Discussion

TGF-β is activated by several factors, such as pH [18], reactive oxygen species [19], thrombospondin-1 [20] and integrin [21–25]. MMPs such as MMP2 and MMP9 also activate TGF-β through proteolytic degradation of the latent TGF-β complex [25,26]. Active TGF-β is present in the extracellular matrix of secretory-stage enamel and induces the differentiation of human periodontal ligament cells [9]. In the present study, we decided to use *Mmp20*$^{-/-}$ mice for a better understanding of *in vivo* TGF-β activation by MMP20 [27] and demonstrated that the TGF-β activity in *Mmp20*$^{-/-}$ mice was significantly lower than that in *Mmp20*$^{+/+}$ mice and *Mmp20*$^{+/-}$ mice at days 5 and 11. We interpret this finding as evidence that MMP20 is one of the activators for TGF-β in the enamel matrix *in vivo*.

TGF-β is activated by the αvβ6 integrin [23] which is expressed by ameloblasts. It plays an important role in regulating amelogenin deposition and the deletion of this integrin causes severe abnormalities in enamel development with the accumulation of amelogenin [28]. Although MMP20 is one of the key activators of TGF-β *in vivo*, its activity has been detected in enamel samples of *Mmp*20 null mice. This finding suggests that TGF-β in enamel matrix is also activated by another factor other than MMP20 such as αvβ6 integrin.

TGF-β signaling is partially mediated by regulating *Mmp20* mRNA expression [29]. In porcine dental pulp tissue, active-form of TGF-β1 enhances *Mmp20* mRNA expression [27]. Both TGF-β1 and TGF-β3 were predominant in enamel but TGF-β2 had a trace concentration. Moreover, the expression of both TGF-β1 and TGF-β3 decreased in *Mmp20*$^{+/-}$ and *Mmp20*$^{-/-}$ mice, and in particular, TGF-β3 dramatically decreased in mice at day 11. This finding suggests that the autocrine signaling of TGF-β through MMP20 is not as well-regulated as other reactions related to MMP20 in secretory-stage enamel followed by early maturation-stage enamel.

TGF-β inhibits the growth of cells such as epithelial cells, endothelial cells, embryonic fibroblasts and hematopoietic cells by inhibiting cyclin dependent kinase activities associated with the G1 to S phase progression [30–35]. mHAT9d is a mouse inner enamel epithelial cell line derived from the apical bud region of a mouse incisor [16,36]. We demonstrated that three TGF-β isoforms inhibited cell growth in mHAT9d cells and that TGF-β3 was the most suppressive at day 2 in particular. Considering that the cell population doubling time was increased by TGF-β3 (approximately 2.0 to 2.5-fold) over that induced by TGF-β1 and TGF-β2, our finding suggests that the cell growth in mHAT9d cells is regulated in TGF-β isoform-specific manner.

A transcriptome study of laser micro dissected ameloblasts obtained from day 5 and days 11–12 mouse first molars showed that 373 genes were more highly expressed in secretory-stage ameloblasts, whereas 614 genes were increased in maturation-stage ameloblasts [37]. We analyzed mRNA levels of the widely known marker genes of secretory- and maturation-stage

ameloblasts (see "Selected genes for RT-qPCR analysis" in the Appendix A). Our RT-qPCR analysis at day 10 after culture in the absence of TGF-β isoforms demonstrated that most maturation-stage genes such as *Klk4*, *Amtn*, *Odam*, *Atp6v1e1* and *Car2* were expressed in mHAT9d cells, but trace levels of *Amel*, *Enam*, *Ambn* and *Mmp20* were detected. This result suggests that the mHAT9d cells used in the present study show maturation stage characteristics.

TGF-β1, TGF-β2 and TGF-β3 have similar functions in mammals [7,8]. TGF-β isoforms are expressed by ameloblasts throughout amelogenesis, but their expression levels vary depending upon the differentiation stage. We demonstrated that the mRNA expression levels of the TGF-β isoforms were predominantly in the order of TGF-β2 >> TGF-β1 > TGF-β3 in mHAT9d cells. However, our ELISA analysis showed that TGF-β2 was barely detected in the mouse enamel matrix at both day 5 and day 11. The reason for this contradiction between cultured cells and the matrix is currently unknown.

Three TGF-β isoforms bind to two TGF-β type I receptors (TGFBR1) and two TGF-β type II receptors (TGFBR2) to form a heterodimeric complex involved in signal transduction. We previously showed the presence of the mRNA of the TRFBR1 transcript through secretory-, transition- and maturation-stages, although its level at the secretory-stage was higher than that at other two stages [10]. TGF-β isoforms have indicated that TGF-β1 is closely related to the differentiation of enamel organ cells and the initiation of matrix secretion; TGF-β2, to cellular differentiation; and TGF-β3, to mineral maturation matrix [38]. In other areas of research such as embryogenesis, wound healing and palatal suture fusion TGF-β isoforms (especially TGF-β1 and TGF-β3) have been shown to possess distinct and opposing effects *in vivo* [39–42]. In the present study, we demonstrated that three TGF-β isoforms specifically regulate gene expression in maturation-stage ameloblasts; in particular, it is very interesting that TGF-β3 downregulated the expression of most of the genes, such as *Amtn*, *Odam*, *Fam83h*, *Wdr72*, *Car2* and *Alp*, but upregulated the expression of *Klk4*. These findings suggest that an antagonistic relationship and/or a different pathway (*i.e.* Smad and non-Smad) may exist among TGF-β isoforms in ameloblasts.

In general, apoptosis is a process of programmed cell death that takes place throughout the life of an organism. Approximately 25% of ameloblasts undergo apoptosis in the short transition stage, and approximately another 25% of ameloblasts are lost throughout the maturation stage [5]. Both *in vitro* and *in vivo* studies have shown that TGF-β1 induces ameloblast apoptosis during the maturation stage [43]. A histological study using ameloblast-specific TGF-β receptor type II conditional knockout (cKO) mice at postnatal day 7 showed that TUNEL-positive ameloblasts were found in both control and cKO mice but that the number of TUNEL-positive cells was almost the same in both genotypes, suggesting that there are few differential effects of TGF-β signaling on ameloblasts at the secretory stage [44]. We demonstrated that three TGF-β isoforms induced apoptosis of ameloblasts and that, in particular, TGF-β3 caused extensive apoptosis of mHAT9d cells. Considering the results of the MTS assay and RT-qPCR analysis, this finding suggests that TGF-β3, unlike TGF-β1 and TGF-β2, exhibits different behaviors with respect to cell proliferation, gene expression and apoptosis in mHAT9d cells.

Endocytosis of degraded proteins occurs throughout all stages of enamel formation. Enamel proteins are sequentially processed and degraded into cleaved fragments, which are internalized by ameloblasts [45]. In the secretory stage, degraded enamel proteins are resorbed *via* vesicles including stippled materials, which originate from ameloblast-membrane infoldings of Tomes' process [17,46]. In the maturation stage, degraded enamel proteins permeate the area between convoluted tubules of the basal lamina followed by uptake *via* vesicles originating from membrane invaginations of ruffle-ended ameloblasts [17]. Amelogenin interacts with the transmembrane proteins CD63 and lysosome-associated membrane protein 1 (LAMP1) to perform endocytosis, and residues of PLSPILPELPLEAW in the amelogenin structure are required for binding to CD63 and LAMP1 [47]. In a cellular uptake study using porcine enamel matrix proteins, amelogenin colocalized with LAMP1 in the perinuclear region of mouse preosteoblasts MC3T3-E1 and ameloblast-like LS8 cells [48]. The P103 amelogenin is a cleavage product of the P173 original amelogenin in the secretory-stage enamel (Appendix Fig. A6). The active-form of TGF-β1 binds to this amelogenin to maintain its activity and moves in the liquid phase to bind to TGF-β receptor on the surface of ameloblasts [10]. We selected P103 amelogenin for the uptake study into mHAT9d cells. We demonstrated that P103 amelogenin lacking CD63 and LAMP1 binding sites (Appendix Fig. A6) was localized in the perinuclear region of mHAT9d cells and that both TGF-β1 and TGF-β3 were associated with the promotion and sustainability of P103 amelogenin uptake into cells. Considering that TGF-β activity is regulated by two distinct endocytic pathways, namely, the clathrin- and caveolar/lipid-raft-mediated pathways [49], our finding suggests that the regulation system of endocytosis for amelogenin depends on TGF-β without involving CD63 and LAMP1 interactions in the cell.

5. Conclusions

Based on the fundamental knowledge obtained in the present study, we propose that TGF-β is regulated in an isoform-specific manner to exert multiple biological functions such as cell proliferation, gene expression related to the structure of basal lamina/ameloblasts and mineral ion transport, apoptosis, and endocytosis for maturation-stage ameloblasts. Further studies are necessary to elucidate the TGF-β signaling pathway with respect to each TGF-β isoform during amelogenesis.

Acknowledgments

We thank Dr. Hidemitsu Harada from the Division of Developmental Biology and Regenerative Medicine, Department of Anatomy, Iwate Medical University (Morioka, Iwate, Japan), who provided the mHAT9d cells. We also thank Drs. Yoshinobu Asada from the Department of Pediatric Dentistry and Ichiro Saito from the Department of Pathology at the School of Dental Medicine, Tsurumi University, and James P. Simmer from the Department of Biologic and Materials Sciences at the University of Michigan School of Dentistry, for their support. This study was supported by a JSPS KAKENHI Grant-in-Aid for Scientific Research (C) (18K09627, 17K11975 and 16K11844), a Grant-in-Aid for Research Activity Start-up (17H07198) and the MEXT-Supported Program for the Strategic Research Foundation at Private Universities (S1511018). The authors acknowledge the Mutant Mouse Regional Resource Center U42OD010918 as the source of the *Mmp20* knockout mice used in this study.

Ethical approval

All animal experiments were approved by the Institutional Animal Care Committee and the Recombination DNA Experiment and Biosafety Committee of the Tsurumi University School of Dental Medicine. Mouse experiments using *Mmp20*$^{+/+}$ and *Mmp20*$^{-/-}$ mice were performed in accordance with protocols approved by the Institutional Animal Care and Use Committee at The Forsyth Institute.

Conflict of interest

The authors declare no potential conflicts of interest with respect to the authorship and/or publication of this article.

CRediT authorship contribution statement

Miu Okubo: Conceptualization, Data curation, Formal analysis, Investigation, Writing - original draft. **Risako Chiba:** Data curation, Formal analysis, Investigation. **Takeo Karakida:** Data curation, Formal analysis, Investigation. **Hajime Yamazaki:** Data curation, Formal analysis. **Ryuji Yamamoto:** Data curation, Investigation, Software. **Saeko Kobayashi:** Formal analysis. **Takahiko Niwa:** Formal analysis. **Henry C. Margolis:** Investigation. **Takatoshi Nagano:** Resources. **Yasuo Yamakoshi:** Conceptualization, Data curation, Formal analysis, Investigation, Resources, Writing - original draft, Writing - review & editing. **Kazuhiro Gomi:** Conceptualization, Writing - original draft, Writing - review & editing

Appendix A

See Appendix Figs. A1–A6.

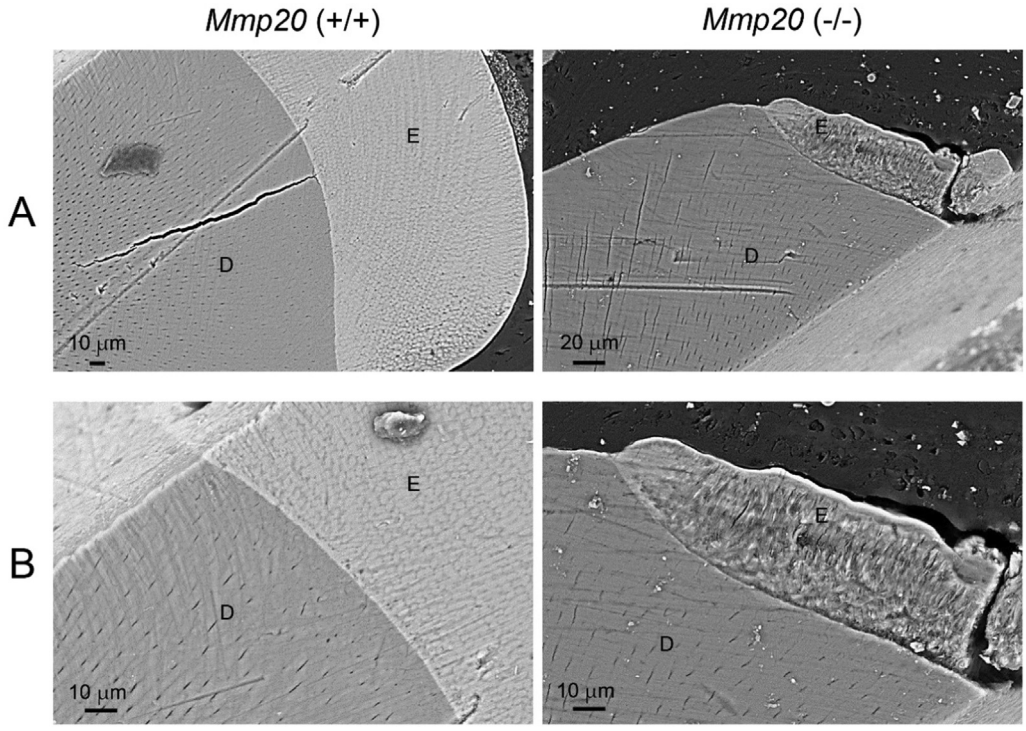

Fig. A1. Backscattered scanning electron microscopy (bSEM) analysis of 3-month-old wild-type (*Mmp20*(+/+)) and Mmp20 null (*Mmp20*(-/-)) mice. **(A)** Magnification × 1000. **(B)** Magnification × 2000. The enamel layers of *Mmp20*(+/+) mice possess normal thickness and rod decussation patterns, whereas the enamel layers of *Mmp20*(-/-) mice are poorly mineralized and show irregular and disordered enamel rods. E: enamel, D: dentin.

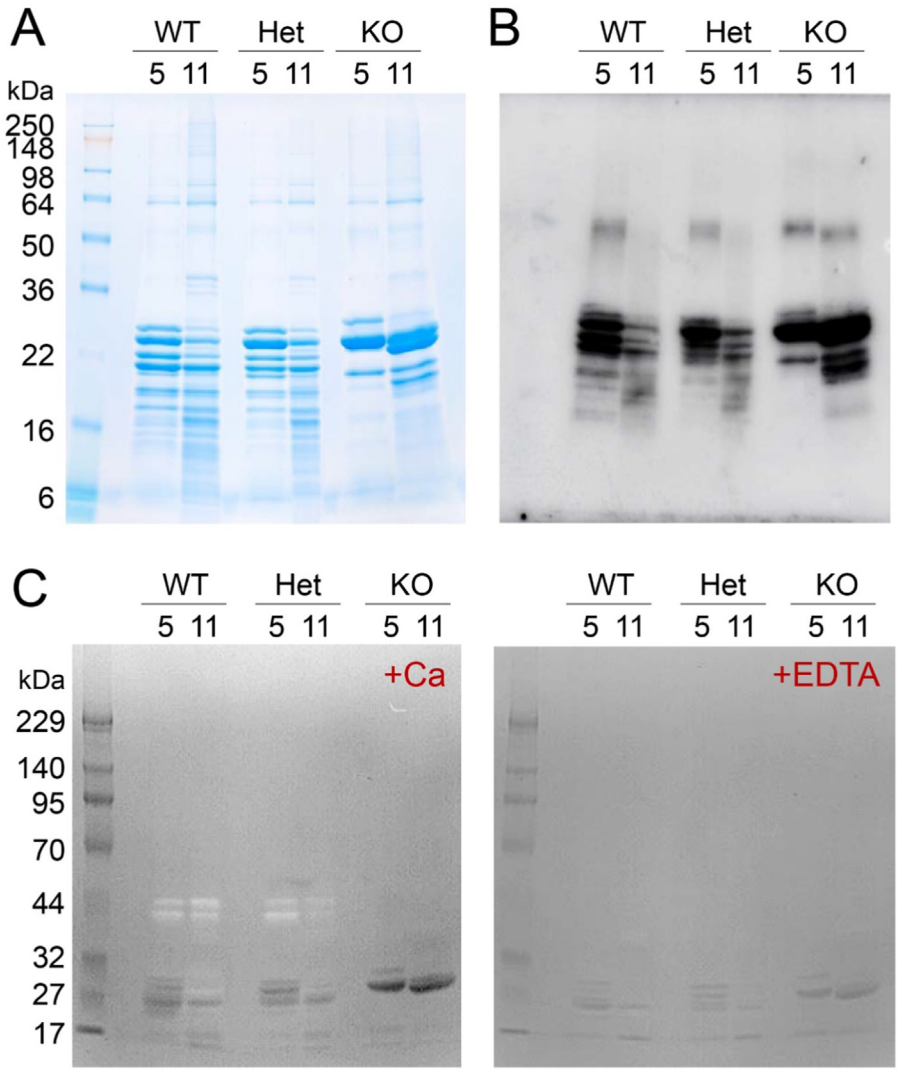

Fig. A2. Protein characterization at days 5 (5) and 11 (11) in wild-type (WT), matrix metalloproteinase 20 (*Mmp20*) heterozygous (Het) and *Mmp*20 null (KO) mice. **(A)** SDS-PAGE (15% gel) stained with Simply Blue. **(B)** Western blot using a specific antibody against mouse amelogenin. **(C)** A casein zymogram of protein fractions incubated with $CaCl_2$ (left) or with EDTA (right). We normalized the amount of protein applied per lane to the SDS-PAGE gel for each genotype on a per-tooth basis. The number of teeth used for each group, the total milligrams of protein extracted, and the milligrams of protein extracted per tooth are listed in Appendix Table A2.

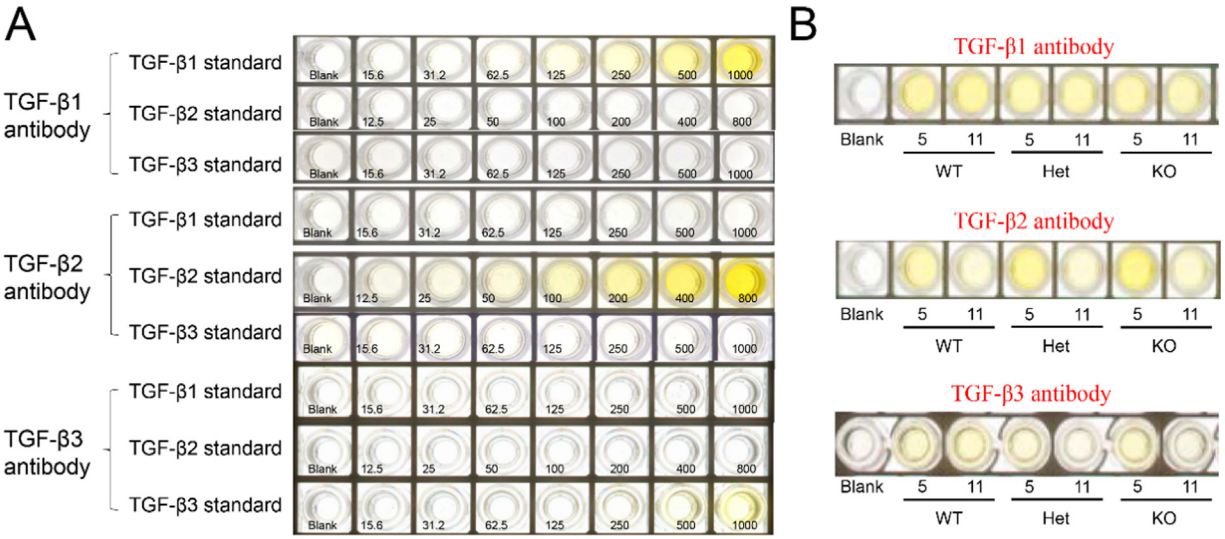

Fig. A3. ELISA for TGF-β isoforms. **(A)** Cross-matching of each TGF-β antibody against other TGF-β isoforms (TGF-β standard). Numbers indicate a concentration (pg/mL) of each TGF-β isoform standard. **(B)** ELISA for the detection of TGF-β isoforms at days 5 (5) and 11 (11) from wild-type (WT), matrix metalloproteinase 20 (*Mmp20*) heterozygous (Het) and *Mmp*20 null (KO) mice. Following the creation of calibration curve for each TGF-β isoforms, the concentration of each TGF-β isoforms was calculated and bar graph shown in main Fig. 1B. TGF-β1 (left), TGF-β2 (middle) and TGF-β3 (right). Blank: antibody only without protein samples.

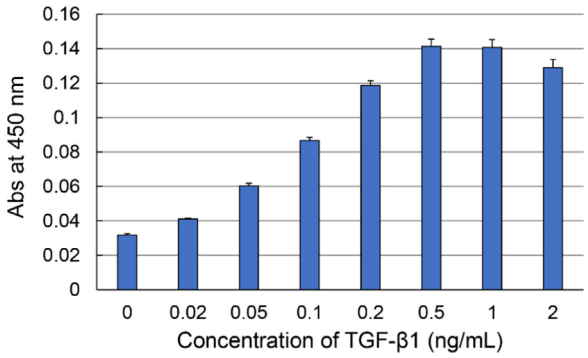

Fig. A4. Maximum effective concentration of human recombinant TGF-β1 (Cell Signalling Technology) for ALP-inducing activity in HPDL cells.

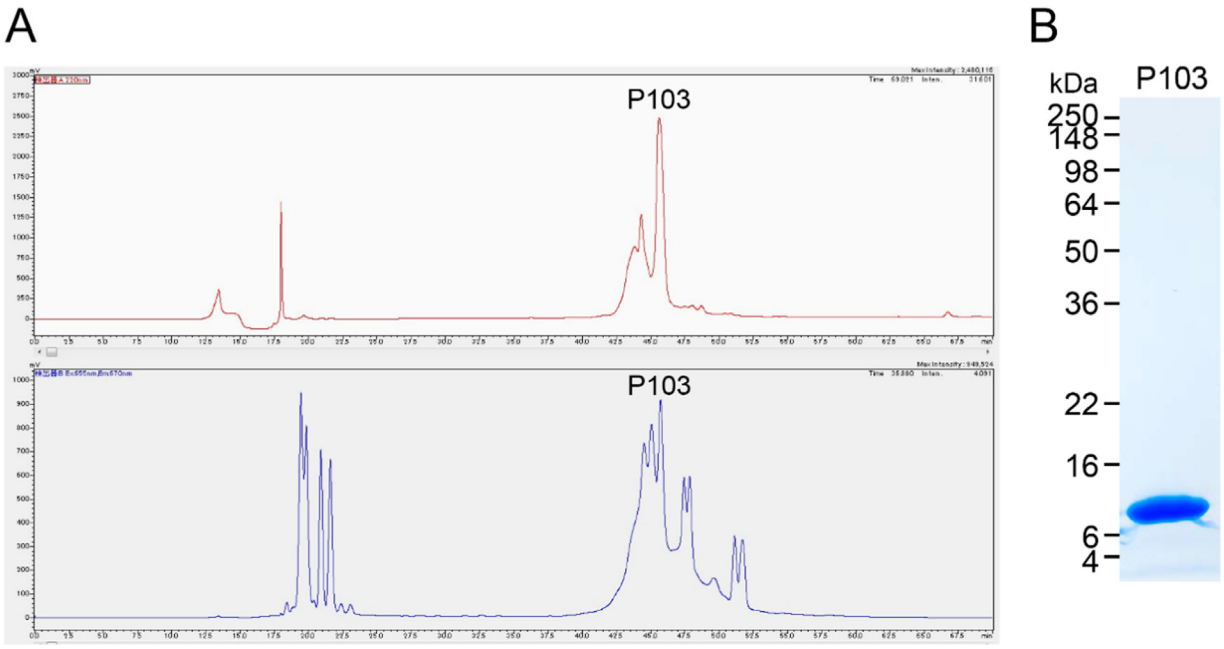

Fig. A5. Purification of HyLyte Fluor 647-labeled P103 amelogenin by reverse phase-high performance chromatography. **(A)** Upper and lower panels show the UV (at 230 nm) (red) and fluorescent (at Ex 655 nm and Em 670 nm) (blue) chromatograms for HyLyte Fluor 647-labeled P103 amelogenin, respectively. **(B)** SDS-PAGE (5–20% gradient gel) stained with Simply Blue showing a purified HyLyte Fluor 647-labeled P103 amelogenin.

```
M180:MPLPPHPGSPGYINLSYEVLTPLKWYQSMIRQPHPSYGYEPMGGWLHHQIIPVLSQQHPPSHT
P173:MPLPPHPGHPGYINFSYEVLTPLKWYQNMIRHPYTSYGYEPMGGWLHHQIIPVVSQQTPQSHA
P103:                                                LHHQIIPVVSQQTPQSHA

M180:LQPHHHLPVVPAQQPVAPQQPMMPVPGHHSMTPTQHHQPNIPPSAQQPFQQPFQPQAIPPQSH
P173:LQPHHHIPMVPAQQPGIPQQPMMPLPGQHSMTPTQHHQPNLPLPAQQPFQPQPVQ----PQPH
P103:LQPHHHIPMVPAQQPGIPQQPMMPLPGQHSMTPTQHHQPNLPLPAQQPFQPQPVQ----PQPH

M180:QPMQPQSPLHPMQPLAPQPPLPPLFSMQPLSPILPELPLEAWPATDKTKREEVA(180)
P173:QPLQPQSPMHPIQPLLPQPPLPPMFSMQ---SLLPDLPLEAWPATDKTKREEVD(173)
P103:QPLQPQSPMHPIQPLLPQPPLPPMFS(103)
```

Fig. A6. Amino acid sequences of murine and porcine amelogenins. Numbers in parenthesis indicate the number of amino acid residues. A dotted line indicates the lacked sequence. The bold red indicates the binding site to the transmembrane proteins CD63 and lysosome-associated membrane protein 1 (LAMP1) to perform endocytosis. M180: murine amelogenin. P173: major porcine amelogenin. P103: water-soluble amelogenin cleaved from P173 amelogenin by MMP20.

See Appendix Tables A1 and A2.

Table A1
Selected primers, size of amplified product (bp) for RT-qPCR analysis shown in main Fig. 3 and Table 1.

Gene		Sequence (5'- > 3')	bp	Gene		Sequence (5'- > 3')	bp
Tgf-β1	F	TGGGACCCTGCCCCTATATT	143	*Amtn*	F	CGCACATACTCTCCCGTTCA	101
	R	CACGTAGTAGACGATGGGCA			R	CACCCTGAGCTCCAAGTTGT	
Tgf-β2	F	GAAGACCCCACATCTCCTGC	134	*Odam*	F	GCACAGCTCCAGAAACTCCT	125
	R	GGCGAAGGCAGCAATTATCC			R	GCTGGGCTTTGGTGAAGTTG	
Tgf-β3	F	GATCACCACAACCCACACCT	150	*Fam83h*	F	TTCCAAGGCACAGAGGTCAC	211
	R	ATAAAGGGGGCGTACACAGC			R	GGGCGTTCATTTCATCCAGC	
Mmp20	F	GGCGAGATGGTGGCAAGAG	166	*Wdr72*	F	AAGGGGACTGTCTACCCTCA	150
	R	CTGGGAAGAGGCGGTAGTT			R	CCACAACGTTATTCTCCCCGA	
Amel	F	ATCCCTGAGCTTCAGACAGAAA	107	*Car2*	F	AACCGGATGGATTGGCTGTT	128
	R	CATAGCAAAAGCTGCTCCCAG			R	GAAGTTAGCAAAGGCCGCAC	
Enam	F	TGCAGAAATCCGACTTCTCCT	114	*Atp6v1e1*	F	CTCAGAGCAAGGGATGACCTC	94
	R	CATCTGGAATGGCATGGCA			R	GCACTTGGTAACGGGTCGTA	
Ambn	F	ATGAAGGGCCTGATCCTGTTC	130	*Alp*	F	GGGCAATGAGGTCACATCCA	85
	R	GTCTCATTGTCTCAAGGCTCAAA			R	GTGGTTCACCCGAGTGGTAG	
Klk4	F	TGACCCTGTGTACCACCTCA	130	*Gapdh*	F	CCATCACCATCTTCCAGGAG	346
	R	TTGTCCCATAGACACGAGCC			R	ACAGTCTTCTGGGTGGCAGT	

Note: The reactions ran for 45 cycles, with denaturing at 95 °C for 10 seconds, annealing at 60 °C for 10 seconds, and extension at 72 °C for 15 seconds. F: forward and R: reverse.

Table A2
Number of teeth used for each group, total amount of protein extracted, and amount protein extracted per a tooth obtained from *Mmp20*(+/+), *Mmp20*(+/-) and *Mmp20(-/-)* mice for the characterization by SDS-PAGE, Western blot and zymography shown in Appendix Fig. A2.

	Mmp20(+/+) (WT)	*Mmp20*(+/-) (Het)	*Mmp20(-/-)* (KO)
Day 5 total amount	9.22 mg/39 teeth	13.92 mg/48 teeth	6.62 mg/32 teeth
amount/one tooth	0.236 mg	0.290 mg	0.207 mg
Day 11 total amount	44.7 mg/39 teeth	50.75 mg/48 teeth	20.22 mg/24 teeth
amount/a tooth	1.146 mg	1.057 mg	0.843 mg

Selected genes for RT-qPCR analysis

In the secretory stage, ameloblasts are polarized columnar cells, and enamel proteins such as amelogenin, ameloblastin, and enamelin are expressed during the secretory stage of ameloblasts, in addition to MMP20 as described above [50]. In the maturation stage, ameloblasts alternate between a ruffle-ended and smooth-ended morphology [51], and enamel proteins are degraded by kallikrein 4, which is a key serine protease expressed in maturation-stage ameloblasts [52]. Maturation-stage ameloblasts are bound to enamel by a basal lamina-like structure [53], and both amelotin and ODAM are localized to the ameloblast basal lamina [54,55]. In addition to these extracellular proteins, intracellular proteins such as FAM83H and WDR72 are also expressed in ameloblasts. *In situ* hybridization analysis has shown that *FAM83H* is highly expressed in presecretory- and secretory-stage ameloblasts [56]. Moreover, the expression of *AA3409316*, a mouse homolog of human *FAM83H*, has been detected in the ameloblasts of a 3-week-old mouse anterior tooth [57]. An immunohistochemical study has shown that the WDR72-positive signal in mouse incisors is increased in maturation-stage ameloblasts compared with that in secretory-stage ameloblasts [58]. Maturation-stage ameloblasts also show increased mineral ion transport. V-ATPase plays a key role in maintaining cellular pH homeostasis [59]. It is a multisubunit protein complex, and *Atp6v1e1* is the highest expressed in rat maturation-stage ameloblasts [60]. Carbonic anhydrase II (*Car2*) is also expressed at the beginning of the maturation stage [59]. Alkaline phosphatase has been detected in the stratum intermedium of the enamel organ at the secretory stage, whereas it has been present in ameloblasts at the maturation stage [61]. Thus we selected above genes and analysed mRNA level with qPCR analysis.

References

[1] Smith CE, Pompura JR, Borenstein S, Fazel A, Nanci A. Degradation and loss of matrix proteins from developing enamel. Anat Rec 1989;224:292–316.
[2] Smith CE, Nanci A. Protein dynamics of amelogenesis. Anat Rec 1996;245: 186–207.
[3] Lacruz RS, Brookes SJ, Wen X, Jimenez JM, Vikman S, Hu P, et al. Adaptor protein complex 2 (AP-2) mediated, clathrin-dependent endocytosis, and related gene activities, are a prominent feature during maturation stage amelogenesis. J Bone Miner Res 2013;28:672–87.
[4] Sasaki T, Higashi S. A morphological, tracer and cytochemical study of the role of the papillary layer of the rat-incisor enamel organ during enamel maturation. Arch Oral Biol 1983;28:201–10.
[5] Smith CE, Warshawsky H. Quantitative analysis of cell turnover in the enamel organ of the rat incisor. Evidence for ameloblast death immediately after enamel matrix secretion. Anat Rec 1977;187:63–98.
[6] Kubiczkova L, Sedlarikova L, Hajek R, Sevcikova S. TGF-β – an excellent servant but a bad master. J Transl Med 2012;10:183.
[7] Massague J. Receptors for the TGF-β family. Cell 1992;69:1067–70.
[8] Kingsley DM. The TGF-β superfamily: new members, new receptors, and new genetic tests of function in different organisms. Genes Dev 1994;8:133–46.
[9] Nagano T, Oida S, Suzuki S, Iwata T, Yamakoshi Y, Ogata Y, et al. Porcine enamel protein fractions contain transforming growth factor-β1. J Periodontol 2006;77:1688–94.
[10] Kobayashi-Kinoshita S, Yamakoshi Y, Onuma K, Yamamoto R, Asada Y. TGF-β1 autocrine signalling and enamel matrix components. Sci Rep 2016;6:33644.
[11] Caterina JJ, Skobe Z, Shi J, Ding Y, Simmer JP, Birkedal-Hansen H, et al. Enamelysin (matrix metalloproteinase 20)-deficient mice display an amelogenesis imperfecta phenotype. J Biol Chem 2002;277:49598–604.
[12] Yamakawa S, Niwa T, Karakida T, Kobayashi K, Yamamoto R, Chiba R, et al. Effects of Er:YAG and diode laser irradiation on dental pulp cells and tissues. Int J Mol Sci 2018:19.
[13] Yamakoshi Y, Hu JC-C, Ryu OH, Tanabe T, Oida S, Fukae M, et al. A comprehensive strategy for purifying pig enamel proteins. In: Kobayashi I, Ozawa H, editors. Biomineralization: formation, diversity, evolution and application. Proceedings of the 8th international symposium on biomineralization, Niigata, Jpn, Sept 25–28, 2001. Hadano, Jpn: Tokai University Press; 2003, p. 326–32.
[14] Hu Y, Hu JC, Smith CE, Bartlett JD, Simmer JP. Kallikrein-related peptidase 4, matrix metalloproteinase 20, and the maturation of murine and porcine enamel. Eur J Oral Sci 2011;119(Suppl. 1):S217–25.
[15] Yamakoshi Y, Richardson AS, Nunez SM, Yamakoshi F, Milkovich RN, Hu JC, et al. Enamel proteins and proteases in Mmp20 and Klk4 null and double-null mice. Eur J Oral Sci 2011;119(Suppl. 1):S206–16.
[16] Otsu K, Kishigami R, Fujiwara N, Ishizeki K, Harada H. Functional role of rho-kinase in ameloblast differentiation. J Cell Physiol 2011;226:2527–34.
[17] Pham CD, Smith CE, Hu Y, Hu JC, Simmer JP, Chun YP. Endocytosis and enamel formation. Front Physiol 2017;8:529.
[18] Lyons RM, Keski-Oja J, Moses HL. Proteolytic activation of latent transforming growth factor-β from fibroblast-conditioned medium. J Cell Biol 1988;106:1659–65.
[19] Barcellos-Hoff MH, Dix TA. Redox-mediated activation of latent transforming growth factor-β 1. Mol Endocrinol 1996;10:1077–83.
[20] Schultz-Cherry S, Murphy-Ullrich JE. Thrombospondin causes activation of latent transforming growth factor-β secreted by endothelial cells by a novel mechanism. J Cell Biol 1993;122:923–32.
[21] Annes JP, Munger JS, Rifkin DB. Making sense of latent TGFβ activation. J Cell Sci 2003;116:217–24.
[22] Munger JS, Harpel JG, Giancotti FG, Rifkin DB. Interactions between growth factors and integrins: latent forms of transforming growth factor-β are ligands for the integrin αvβ1. Mol Biol Cell 1998;9:2627–38.
[23] Munger JS, Huang X, Kawakatsu H, Griffiths MJ, Dalton SL, Wu J, et al. The integrin αvβ6 binds and activates latent TGF β1: a mechanism for regulating pulmonary inflammation and fibrosis. Cell 1999;96:319–28.
[24] Shi M, Zhu J, Wang R, Chen X, Mi L, Walz T, et al. Latent TGF-β structure and activation. Nature 2011;474:343–9.
[25] Stetler-Stevenson WG, Aznavoorian S, Liotta LA. Tumor cell interactions with the extracellular matrix during invasion and metastasis. Annu Rev Cell Biol 1993;9:541–73.
[26] Yu Q, Stamenkovic I. Cell surface-localized matrix metalloproteinase-9 proteolytically activates TGF-β and promotes tumor invasion and angiogenesis. Genes Dev 2000;14:163–76.
[27] Niwa T, Yamakoshi Y, Yamazaki H, Karakida T, Chiba R, Hu JC, et al. The dynamics of TGF-β in dental pulp, odontoblasts and dentin. Sci Rep 2018;8:4450.
[28] Mohazab L, Koivisto L, Jiang G, Kytomaki L, Haapasalo M, Owen GR, et al. Critical role for alphavbeta6 integrin in enamel biomineralization. J Cell Sci 2013;126:732–44.
[29] Gao Y, Zhang L, Xiang L, Li B, Liu X, Wang Y, et al. Transforming growth factor-β1 regulates expression of the matrix metalloproteinase 20 (Mmp20) gene through a mechanism involving the transcription factor, myocyte enhancer factor-2C, in ameloblast lineage cells. Eur J Oral Sci 2014;122:114–20.
[30] Heldin CH, Miyazono K, ten Dijke P. TGF-β signalling from cell membrane to nucleus through SMAD proteins. Nature 1997;390:465–71.
[31] Massague J. TGF-β signal transduction. Annu Rev Biochem 1998;67:753–91.
[32] Roberts AB, Sporn MB. Physiological actions and clinical applications of transforming growth factor-β (TGF-β). Growth Factors 1993;8:1–9.
[33] Roberts AB. Molecular and cell biology of TGF-β. Miner Electrolyte Metab 1998;24:111–9.
[34] Derynck R, Zhang YE. Smad-dependent and Smad-independent pathways in TGF-β family signalling. Nature 2003;425:577–84.
[35] Moustakas A. Smad signalling network. J Cell Sci 2002;115:3355–6.
[36] Kawano S, Morotomi T, Toyono T, Nakamura N, Uchida T, Ohishi M, et al. Establishment of dental epithelial cell line (HAT-7) and the cell differentiation dependent on Notch signaling pathway. Connect Tissue Res 2002;43:409–12.
[37] Simmer JP, Richardson AS, Wang SK, Reid BM, Bai Y, Hu Y, et al. Ameloblast transcriptome changes from secretory to maturation stages. Connect Tissue Res 2014;55(Suppl. 1):S29–32.
[38] Sassa Benedete AP, Sobral AP, Lima DM, Kamibeppu L, Soares FA, Lourenco SV. Expression of transforming growth factor-β 1, -β 2, and -β 3 in human developing teeth: immunolocalization according to the odontogenesis phases. Pediatr Dev Pathol 2008;11:206–12.
[39] Nacamuli RP, Song HM, Fang TD, Fong KD, Mathy JA, Shi YY, et al. Quantitative transcriptional analysis of fusing and nonfusing cranial suture complexes in mice. Plast Reconstr Surg 2004;114:1818–25.
[40] Greenwald JA, Mehrara BJ, Spector JA, Warren SM, Crisera FE, Fagenholz PJ, et al. Regional differentiation of cranial suture-associated dura mater in vivo and in vitro: implications for suture fusion and patency. J Bone Miner Res 2000;15:2413–30.
[41] Fagenholz PJ, Warren SM, Greenwald JA, Bouletreau PJ, Spector JA, Crisera FE, et al. Osteoblast gene expression is differentially regulated by TGF-β isoforms. J Craniofac Surg 2001;12:183–90.
[42] Leonard CM, Fuld HM, Frenz DA, Downie SA, Massague J, Newman SA. Role of transforming growth factor-β in chondrogenic pattern formation in the embryonic limb: stimulation of mesenchymal condensation and fibronectin gene expression by exogenenous TGF-β and evidence for endogenous TGF-β-like activity. Dev Biol 1991;145:99–109.
[43] Tsuchiya M, Sharma R, Tye CE, Sugiyama T, Bartlett JD. Transforming growth factor-β1 expression is up-regulated in maturation-stage enamel organ and may induce ameloblast apoptosis. Eur J Oral Sci 2009;117:105–12.
[44] Cho A, Haruyama N, Hall B, Danton MJ, Zhang L, Arany P, et al. TGF-β regulates enamel mineralization and maturation through KLK4 expression. PLoS One 2013;8:e82267.
[45] Bartlett JD, Smith CE. Modulation of cell-cell junctional complexes by matrix metalloproteinases. J Dent Res 2013;92:10–7.
[46] Nanci A, Slavkin HC, Smith CE. Immunocytochemical and radioautographic evidence for secretion and intracellular degradation of enamel proteins by ameloblasts during the maturation stage of amelogenesis in rat incisors. Anat Rec 1987;217:107–23.
[47] Zou Y, Wang H, Shapiro JL, Okamoto CT, Brookes SJ, Lyngstadaas SP, et al. Determination of protein regions responsible for interactions of amelogenin with CD63 and LAMP1. Biochem J 2007;408:347–54.
[48] Shapiro JL, Wen X, Okamoto CT, Wang HJ, Lyngstadaas SP, Goldberg M, et al. Cellular uptake of amelogenin, and its localization to CD63, and Lamp1-positive vesicles. Cell Mol Life Sci 2007;64:244–56.
[49] Huang SS, Huang JS. TGF-β control of cell proliferation. J Cell Biochem 2005;96:447–62.
[50] Bartlett JD. Dental enamel development: proteinases and their enamel matrix substrates, 2013. ISRN dentistry; 2013. p. 684607.
[51] Warshawsky H, Smith CE. Morphological classification of rat incisor ameloblasts. Anat Rec 1974;179:423–46.
[52] Simmer JP, Sun X, Yamada Y, Zhang CH, Bartlett JD, Hu JC-C. Enamelysin and kallikrein-4 expression in the mouse incisor. In: Kobayashi I, Ozawa H, editors. Biomineralization: formation, diversity, evolution and application. Proceedings of the 8th international symposium on biomineralization, Niigata, Jpn, Sept 25–28, 2001. Hadano, Jpn: Tokai University Press; 2004, p. 348–52.
[53] Sawada T. Ultrastructural and immunocytochemical characterization of ameloblast-enamel adhesion at maturation stage in amelogenesis in Macaca fuscata tooth germ. Histochem Cell Biol 2015;144:587–96.
[54] Holcroft J, Ganss B. Identification of amelotin- and ODAM-interacting enamel matrix proteins using the yeast two-hybrid system. Eur J Oral Sci 2011;119 (Suppl. 1):S301–6.
[55] Fouillen A, Dos Santos Neves J, Mary C, Castonguay JD, Moffatt P, Baron C, et al. Interactions of AMTN, ODAM and SCPPPQ1 proteins of a specialized basal lamina that attaches epithelial cells to tooth mineral. Sci Rep 2017;7:46683.
[56] Lee MJ, Lee SK, Lee KE, Kang HY, Jung HS, Kim JW. Expression patterns of the Fam83h gene during murine tooth development. Arch Oral Biol 2009;54:846–50.
[57] Kim JW, Lee SK, Lee ZH, Park JC, Lee KE, Lee MH, et al. FAM83H mutations in families with autosomal-dominant hypocalcified amelogenesis imperfecta. Am J Hum Genet 2008;82:489–94.
[58] El-Sayed W, Parry DA, Shore RC, Ahmed M, Jafri H, Rashid Y, et al. Mutations in the beta propeller WDR72 cause autosomal-recessive hypomaturation amelogenesis imperfecta. Am J Hum Genet 2009;85:699–705.
[59] Josephsen K, Takano Y, Frische S, Praetorius J, Nielsen S, Aoba T, et al. Ion transporters in secretory and cyclically modulating ameloblasts: a new hypothesis for cellular control of preeruptive enamel maturation. Am J Physiol Cell Physiol 2010;299:C1299–307.
[60] Sarkar J, Wen X, Simanian EJ, Paine ML. V-type ATPase proton pump expression during enamel formation. Matrix Biol 2016;52–54:234–45.
[61] Wise GE, Fan W. Changes in the tartrate-resistant acid phosphatase cell population in dental follicles and bony crypts of rat molars during tooth eruption. J Dent Res 1989;68:150–6.